JOURNAL OF OPTOELECTRONICS AND ADVANCED MATERIALS Vol. 8, No. 1, February 2006, p. 299 - 303

Structural and optical properties of zinc oxide thin films prepared by spray pyrolysis method

C. GÜMÜŞ, O. M. OZKENDIR, H. KAVAK, Y. UFUKTEPE*
Cukurova Univ. Fac. Sci.& Letters, Dept. Physics, Adana, 01330 Turkey

Polycrystalline ZnO thin films were deposited on a glass substrate by a spray pyrolysis technique using solution of zinc acetate and air as the carrier gas at 400 °C temperature. Optical constants such as refractive index *n* and extinction coefficient *k*, were determined from transmittance spectrum in the ultraviolet-visible-near infrared (UV-VIS-NIR) regions using envelope methods. The films were found to exhibit high transmittance (>90 %), low absorbance and low reflectance in the visible regions. Absorption coefficient α, and the thickness of the film *t* were calculated from interference of transmittance spectra. The energy band gap, and the thickness of the films were evaluated as 3.27 eV and 0.31-0.52 μm respectively. The crystallographic structure of these films was analyzed with x-ray diffractometer. The films were polycrystalline in nature with preferred (002) orientation perpendicular to substrate surface and the grain size estimated to be 40 nm. The extended x-ray absorption fine structure (EXAFS) calculations above the K-edge of Zn in the ZnO thin film have been performed by using real-space multiple scattering of photoelectrons. For ZnO thin films, the values of the correlated mean square relative displacements of nearest-neighbor atoms derived from EXAFS spectra show good agreement with those measured from the x-ray diffraction experiments.

(Received December 8, 2005; accepted January 26, 2006)

Keywords: ZnO, Optical properties, Thin films, Spray pyrolysis, EXAFS

1. Introduction

Zinc oxide (ZnO) is one of transparent conducting oxide (TCO) materials whose thin films attract much interest because of typical properties such as high chemical and mechanical stability in hydrogen plasma, high optical transparency in the visible and near-infrared region [1-3]. Due to these properties ZnO is a promising material for electronic or optoelectronic applications such as solar cells (anti-reflecting coating and transparent conducting materials), gas sensors, liquid crystal displays, heat mirrors, surface acoustic wave devices etc. [4-6]. In addition to the traditional applications ZnO thin films could also be used in integrated optics and gas sensors [7]. Several groups have already done much research on ZnO by use of various film growth techniques, including RF/DC magnetron sputtering [8], chemical bath deposition [9], reactive thermal vacuum evaporation [10], pulsed laser deposition [11], sol-gel method [12] and spray pyrolysis [13,14].

Spray pyrolysis is a useful alternative to the traditional methods for obtaining zinc oxide (ZnO) thin films, because of its simplicity, low cost and minimal waste production. The spray pyrolysis process allows the coating of large surface and it is easy to include in an industrial production line. This technique is also compatible with mass production systems. With spray pyrolysis, the solution is sprayed directly onto the substrate. A stream of gas, e.g. compressed air, can be used to help the atomization of solution through the nozzle.

In this study, ZnO thin films were deposited by the spray pyrolysis technique on glass substrates. The crystallinity and structure of these films were analyzed by X-ray diffraction. Optical properties of the films were also investigated by ultraviolet-visible-near infrared (UV-VIS-NIR) spectrophotometer. The widely used envelope method has been developed for transmittance measurements to evaluate the refractive index, extinction coefficient and absorption coefficient [15]. In the optical transmission spectrum multiple coherent reflections are present due to interference effect and the above parameters can be determined from the envelopes, T_{max} and T_{min} along the interference maxima and minima.

One of the most useful methods allowing study of the local arrangement of atoms is EXAFS. The extended x-ray absorption fine structure showing up above the absorption edges of atoms in molecules, liquids and solids is caused by the interference of the outgoing photoelectron wave with parts of this wave that are backscattered from the neighboring atoms [16]. There has been a great interest in EXAFS since the development of methods for extracting information about local geometrical structures such as bond lengths and coordination numbers from experimental spectra [17]. Whereas the periodicity of the EXAFS oscillation allows us to determine the bond lengths between absorbing and scattering atoms, the amplitudes of the fine structure contain information about the number of atoms that surround the absorbing atom [18].

2. Experimental details

ZnO films were prepared on glass substrates by spray pyrolysis technique. The spray solution was 0.2 M $Zn(CH_3C00)_2{\cdot}2H_20$ (zinc acetate), isopropyl alcohol and distillated water (volume ratio 3 to 1). The carrier gas (compressed air) and solution are fed into a spray nozzle at a pre-adjusted constant atomization pressure. The flow rate of solution was 8 ml/min and the substrate temperature was held constant at 400 °C. The nozzle to substrate distance was 25 cm and diameter of nozzle was 0.3 mm.

The optical properties of ZnO films were carried out with a double beam spectrophotometer (Perkin Elmer Lambda 2S) in the UV/VIS/NIR regions. The optical transmittance at normal incidence was recorded in the wavelength range of 300-1100 nm. Swanepoel's envelope method was employed to evaluate the optical constants such as the refractive index *n*, extinction coefficient *k*, and absorption coefficient α from transmittance spectra [15]. The thickness of ZnO films was determined from interference fringes of transmission data measured over the visible range. The structure and lattice parameters of ZnO films were analyzed by a Rigaku RadB X-ray diffractometer (XRD) with Cu $K_{\alpha 1}$ radiation with λ=1.54056 Å (30 kV, 15 mA, scanning speed = 6°/min).

The full multiple scattering approach was applied to the calculation of Zn K edge EXAFS spectra of hexagonal wurtzite ZnO thin film. In the calculations one Zn atom was selected as an absorber, the thickness of sample was 10 Å and the cluster contains 340 atoms (Zn, O). The calculations are based on different choices of one electron potentials according to Zinc coordination by using FEFF 8.0 code which is based on the real space multiple scattering approach [19,20].

3. Results and discussion

Fig. 1 shows the X-ray diffraction pattern of ZnO thin film deposited at 400 °C only with one sharp and three small peaks present. Diffraction pattern was obtained with 2θ from 10° to 70° at 6° glancing angle. The XRD pattern of the film shows that the film is crystallized in the wurtzite phase and presents a preferential orientation along the c-axis. The result is in agreement with the literature (JCPDF card no 36-1451). The strongest peak observed at 2θ = 34.39° (d = 0.260 nm) can be attributed to the (002) plane of the hexagonal ZnO. The (101), (102) and (103) peaks were also observed at 2θ = 36.17°, 47.47° and 62.78°, respectively but these peaks are of much lower intensity than the (002) peak. The c-axis lattice constant of the ZnO thin film was calculated from XRD data as 5.21 Å. The grain size *g* can be estimated using the Scherrer's formula:

$$g = \frac{0.94\lambda}{\Delta(2\theta)\cos\theta} \qquad (1)$$

where λ is the x-ray wavelength (1.54056 Å), θ and $\Delta(2\theta)$ are the Bragg diffraction angle of the XRD peak in degree and the full width at half maximum (in radian) of (002) diffraction peak respectively [21]. The crystallite size is estimated about 40 nm.

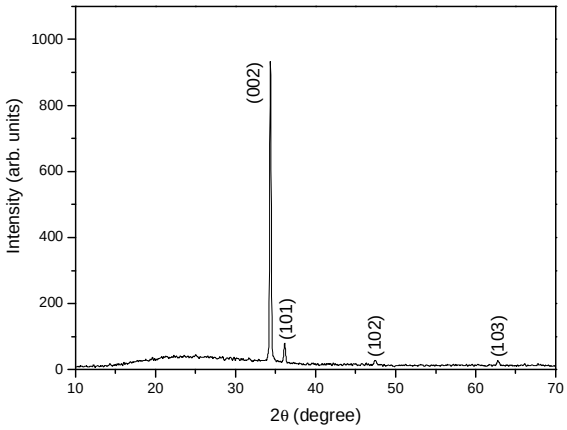

Fig. 1. X-ray diffraction pattern of ZnO film deposited on glass substrate at 400 °C.

Fig. 2 shows the optical transmittance spectrum of ZnO thin film in the wavelength range from 300 to 1100 nm. The films are highly transparent in the visible range of the electromagnetic spectrum with an average transmittance values up to 95 %, and present a sharp ultraviolet cut-off at approximately 380 nm.

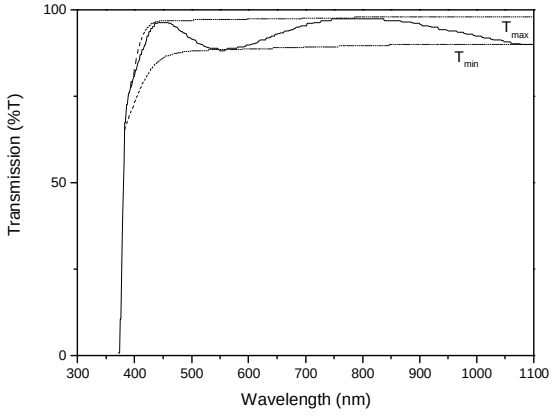

Fig. 2. UV/VIS/NIR transmission curve of ZnO film.

The thickness of the film was calculated using the following relation:

$$t = \frac{\lambda_1\lambda_2}{2[n(\lambda_1)\lambda_2 - n(\lambda_2)\lambda_1]} \qquad (2)$$

where $n(\lambda_1)$ and $n(\lambda_2)$ are the refractive indices at the two adjacent maxima (or minima) at λ_1 and λ_2. The zinc oxide film thickness was found to be 0.52 μm.

The optical constants such as refractive index n and extinction coefficient k were determined from a transmittance spectrum (Fig. 2) using envelope method. The refractive index can be calculated from the following equations:

$$n = \left[N + \left(N^2 - n_s^2 \right)^{1/2} \right]^{1/2},$$

$$N = \frac{\left(n_s^2 + 1 \right)}{2} + 2n_s \frac{\left(T_{\max} - T_{\min} \right)}{T_{\max} T_{\min}}, \qquad (3)$$

where n_s is the refractive index of the substrate. T_{max} and T_{min} are maximum and minimum transmittances at the same wavelength in the fitted envelope curves on the transmittance spectrum. The extinction coefficient can be also calculated by the following equations:

$$k = \frac{\alpha\lambda}{4\pi}, \qquad (4)$$

$$\alpha = \frac{1}{t} \ln \frac{(n-1)(n-n_s)\left[\left(T_{\max} / T_{\min} \right)^{1/2} + 1 \right]}{(n+1)(n-n_s)\left[\left(T_{\max} / T_{\min} \right)^{1/2} - 1 \right]}, \qquad (5)$$

where α is the absorption coefficient and t is the film thickness. λ_1 and λ_2 are the wavelengths at the two adjacent maxima or minima. The optical constants such as refractive index n and extinction coefficient k were determined from a transmittance spectrum by envelope method as explained in the previous section. The variations of refractive index n and extinction coefficient k with wavelength in the region 400 nm-1100 nm are shown in Fig. 3 and Fig. 4.

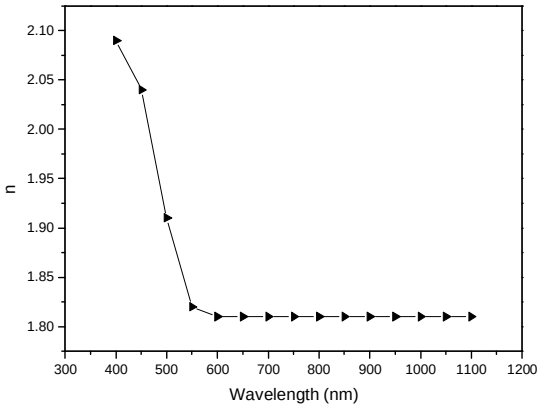

Fig. 3. Plot of refraction index (n) as a function of wavelength.

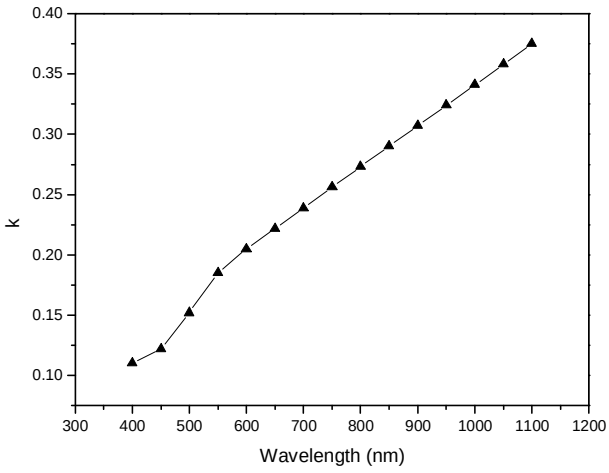

Fig. 4. Plot of extinction coefficient (k) as a function of wavelength.

The absorption coefficient α of ZnO films was determined from transmittance measurements. Since envelope method is not valid in the strong absorption region, the calculation of the absorption coefficient of the film in this region was calculated using the following expression:

$$\alpha = -\frac{1}{t} \ln(T) \qquad (6)$$

where T is the normalized transmittance, t is the film thickness. These absorption coefficients values were used to determine optical energy gap. Fig. 5 shows the plot of α^2 vs. $h\nu$, where α is the optical absorption coefficient and $h\nu$ is the energy of the incident photon. The energy gap (E_g) was estimated by assuming a direct transition between valence and conduction bands from the expression

$$\alpha h\nu = K\left(h\nu - E_g \right)^{1/2} \qquad (7)$$

where K is a constant, E_g is determined by extrapolating the straight line portion of the spectrum to $\alpha h\nu = 0$. From this drawing, the optical energy gap, E_g = 3.27 eV is deduced. This value is slightly smaller than the bulk value of 3.31 eV [22] and in good agreement with previously reported data of ZnO thin film [23]. Table 1 shows some results for the comparison, we conclude that spray pyrolysis is a suitable film deposition technique to obtain very similar properties.

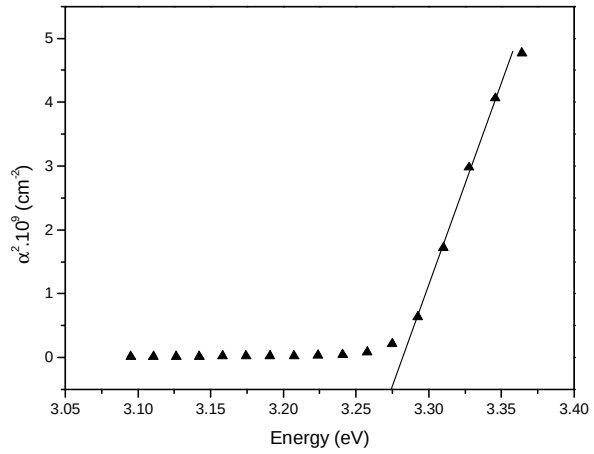

Fig. 5. Plot of α^2 vs. photon energy $h\nu$ for ZnO thin film.

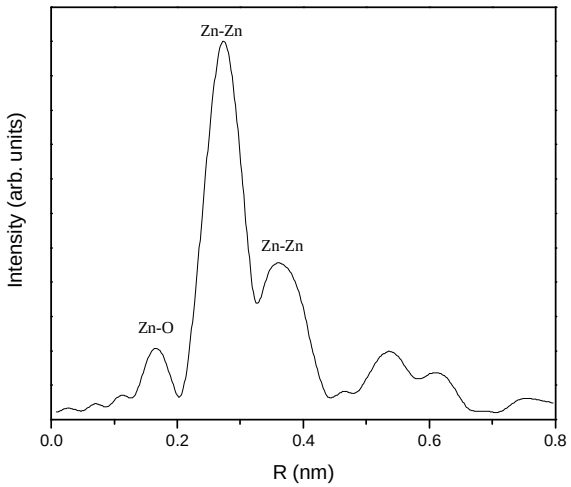

Fig. 6. EXAFS calculated radial distribution function of ZnO thin film.

Table 1.

	Grain size	Band gap	Thickness	Refractive index
Gumus et al.	40 nm	3.27 eV	520 nm	2.09-1.81
[8]	25-48 nm	3.24 eV	450 nm	1.93
[13]	14.6 nm	3.31 eV		
[24]	23 nm		650 nm	
[25]	60 nm	3.11 eV	600 nm	
[26]	30-36 nm	3.28 eV		
[27]		3.20 eV		2-1.87

In addition to the experimental measurements, we also performed EXAFS calculation to determine precise the distances of atomic species from a selected Zinc atom. Fig. 6 displays the Fourier Transform of the energy signals of the scattering intensities, the radial distribution function (RDF). The calculated mean square disorder is $\sigma^2 = 4.506. 10^{-4}$ nm^2. To get the atomic distances precisely, we made fits for the singly scattering paths which are calculated for the EXAFS of ZnO. All distances are determined from the Zn atom located at the origin. The first peak in Fig. 6 shows the distances of 3 Oxygen atoms (Zn-O) at 0.206 nm. The second and the third peak intensities are superposition of different signals from the atomic groups which are located closer to each other. The second peak contains the signals from 5 O atoms at 0.262 nm which is the shortest Zn-Zn bond length and 6 Zn atoms at a distance of 0.328 nm. The third intense peak contains signals from, 3 O atoms at a distance of 0.387 nm, 3 O atoms at 0.393 nm, 3 O atoms at 0.420 nm. The most intense contribution to the signal of third peak comes from the 12 Zn atoms located at 0.420 nm far from the Zn atom at the origin.

4. Conclusion

Highly transparent ZnO thin films were successfully prepared by the spray pyrolysis technique on glass substrate at 400 °C using solution of zinc acetate and air as a carrier gas. The X-ray diffraction analysis showed that film is polycrystalline in nature. The deposited films exhibit excellent crystalline structure with (002) preferential orientation. The grain size is estimated to be 40 nm. The EXAFS calculation for ZnO thin film is in good agreement with the experimental results. Optical measurements show that the film possesses high transmittance over 90 % in the visible region and sharp absorption edge near 380 nm. Envelope method was employed to calculate the refractive index and extinction coefficient as a function of wavelengths. The film has a direct band gap with an optical value of 3.27 eV which is close to the previously reported value (3.28 eV) [26].

References

[1] P. Nunes, B. Fernandes, E. Fortunato, P. Vilarinho, R. Martins, Thin Solid Films **337,** 176 (1999).
[2] D. J. Goyal, C. Agashe, M. G. Takwale, B. R. Marathe, V. G. Bhide, J. Mater. Sci. **27,** 4705 (1992).
[3] A. Sanchez-Juarez, A. Tiburcio-Silver, A. Ortiz, Sol. Energy Mater. Sol. Cells **52,** 301(1998).
[4] L. Chopra, S. Major, D.K. Panday, Thin Solid Films **1021,** 1 (1983).
[5] S. Bose, A. K. Barua, J. Phys.D: Appl. Phys. **32,** 213 (1999).
[6] H. Kim, C. M. Gilmore, Appl. Phys. Lett. **76,** 259 (2000).
[7] G. Feng, D. Li, B. L. Yao, Vacuum **68,** 363 (2003).
[8] A. Moustaghfir, E. Tomasella, S. B. Amor, M. Jacquet, J. Cellier, T. Sauvage, Surf. Coat.

Technol. **174-175,** 193 (2003).
[9] V. R. Shinde, C. D. Lokhandre, R. S. Mane, S. H. Han, Appl. Surf. Sci. **245,** 407 (2005).
[10] J. H. Morgan, D. E. Broide, Can. J. Phys. **60,** 1387 (1982).
[11] V. Craciun, J. Elders, J. G. E. Gardeniers, J. Geretovsky, I. W. Boyd, Thin Solid Films **259,** 1 (1995).
[12] M. Ohyama, H. Kozuka, T. Yoko, Thin Solid Films **306**, 78 (1997).
[13] R. Ayouchi, D. Leinen, F. Martin, M. Gabas, E. Dalchiele, J. R. Ramos-Barrado, Thin Solid Films **426,** 68 (2003).
[14] F. Paraguay, J. Morales, W. Estrada, E. Andrade, M. M. Yoshida, Thin Solid Films **366,** 16 (2000).
[15] D. Minkov, R. Swanepoel, Optical Engineering **32,** 3333 (1993).
[16] J. Stöhr, NEXAFS Spectroscopy, Vol. **25** of Springer Series in Surface Sciences, Springer, Heidelberg, 1992.
17] P. A. Lee, P. H. Citrin, P. Eisenberger, B. M. Kincaid, Rev. of Mod.. Phys. **53,** 769 (1981).
[18] A. Bianconi, in X-ray Absorption: Principles, Applications and Techniques of EXAFS, SEXAFS and XANES, edited by R. Prins and D. C. Koningsberger, Wiley, New York, 1988, p. 573.
[19] A. L. Ankudinov, B. Ravel, J. J. Rehr, S. D. Conradson, Phys. Rev. B **58,** 7565 (1998).
[20] P. J. Durham, J. B. Pendry, C. H. Hodges, Comput. Phys. Commun. **193,** 4425 (1982).
[21] H. P. Klung, L. E. Alexander, X-ray Diffraction Procedures for Polycrystalline and Amorphous Materials, 2nd Edition, Wiley, New York, 1974.
[22] S. Oktik, Prog. Cryst. Growth Charact. **17,** 171 (1988).
[23] F. Paraguay, W. Estrada, D. R. Acosta, E. Andrade, M. M. Yoshida, Thin Solid Films **350,** 192 (1999).
[24] M. Quintana, E. Ricra, J. Rodriguez, W. Estrada, Catalysis Today **76,** 141 (2002).
[25] K. Yoshino, T. Fukushima, M. Yoneta, J. of Mater. Sci.: Mater. in Electronics **16,** 403 (2005).
[26] J-H. Lee, B-W. Yeo, B-O. Park, Thin Solid Films **457,** 333 (2004).
[27] S. E. Demian, J. of Mater. Sci.: Mater. in Electronics **5,** 360 (1994).

* Corresponding author: ufuk@cu.edu.tr